11-1-1999

Piezoelectric Doping in AlInGaN/GaN Heterostructures

M. Asif Khan

J. W. Yang

Grigory Simin
University of South Carolina - Columbia, simin@engr.sc.edu

R. Gaska

M. S. Shur

See next page for additional authors

Author(s)
M. Asif Khan, J. W. Yang, Grigory Simin, R. Gaska, M. S. Shur, and A. D. Bykovski

Piezoelectric doping in AlInGaN/GaN heterostructures

M. Asif Khan, J. W. Yang, G. Simin, R. Gaska, M. S. Shur, and A. D. Bykhovski

Piezoelectric doping in AlInGaN/GaN heterostructures

M. Asif Khan, J. W. Yang, and G. Simin
Department of ECE, University of South Carolina, Columbia, South Carolina 29208

R. Gaska[a]
Sensor Electronics Technology, Inc., Troy, New York 12110

M. S. Shur and A. D. Bykhovski
Department of ECSE and CIEEM, Rensselaer Polytechnic Institute, Troy, New York 12180

We report on the piezoelectric doping and two-dimensional (2D) electron mobility in AlInGaN/GaN heterostructures grown on 6H–SiC substrates. The contribution of piezoelectric doping to the sheet electron density was determined using an In-controlled built-in strain-modulation technique. Our results demonstrate that in strained AlGaN/GaN heterostructures, the piezoelectric field generates at least 50% of the 2D electrons. The strain modulation changes the potential distribution at the heterointerface, which, in turn, strongly affects the 2D electron mobility, especially at cryogenic temperatures. The obtained results demonstrate the potential of strain engineering and piezoelectric doping for GaN-based electronics. © *1999 American Institute of Physics.*
[S0003-6951(99)05344-9]

Strong piezoelectric and pyroelectric effects in AlGaN/GaN heterostructures emerged as powerful tools for the development of a semiconductor doping technique. In contrast to the conventional impurity doping, this method does not introduce any new energy levels, carrier traps, and scattering centers, which strongly affect electrical characteristics of materials and electronic devices. Since our first reports on the piezoelectric doping in AlN–GaN–AlN semiconductor–insulator–semiconductor structures[1] and pyroelectric effect in GaN,[2] a number of reports have been published on the influence of piezoelectric effects on the two-dimensional (2D) electron mobility and sheet density[3–8] in AlGaN/GaN heterostructures. Although the important role of piezoelectric and spontaneous polarization effects in doping of AlN/GaN/InN heterostructures is widely recognized, the key question about the relative contributions of these two effects remains under intense discussion.

The theoretical calculations of Bernardini, Fiorentini, and Vanderbilt[7] and of Bykhovski, Gaska, and Shur[8] predicted the comparable contributions of spontaneous polarization and piezoelectric effects to 2D electron density in AlGaN/GaN heterostructures. However, so far, there is no direct experimental evidence for these estimates. The internal electric fields in pyroelectric materials are usually much smaller than predicted by the theory, which does not account for surface and interface states. In the limiting case, when the surface-state density equals or even exceeds P_s/q, where P_s is spontaneous polarization and q is the electron charge, the charges trapped in surface and/or interface states can cancel the effect of spontaneous polarization, making an internal electric field vanish inside the film.[9] This is often the case in typical ferroelectric materials, which makes a direct determination of the value of spontaneous polarization and its contribution to 2D electron gas near the AlGaN/GaN heterointerface very complicated.

In this letter, we deduce the contribution of piezoelectric doping in AlInGaN/GaN heterostructures by using In-controlled strain engineering and by measuring the properties of 2D electron gas in AlInGaN/GaN heterostructures with different In incorporation.

The epilayer structures for our study were grown by low-pressure metal–organic chemical-vapor deposition on conducting 6H–SiC substrates at 1000 °C and 76 Torr. They consisted of a 100-nm-thick AlN buffer layer followed by approximately 0.5-μm-thick semi-insulating GaN and by a nominally undoped quaternary AlInGaN barrier layer. A different In incorporation in our structures was achieved by keeping constant triethylgallium (TEG) and triethylaluminum (TEA) fluxes while varying the flux of trimethylindium (TMI).

We investigated heterostructures with two different barrier designs which are shown in the inset to Fig. 1. These barrier designs consisted of (i) a uniform AlInGaN layer and (ii) a two-layer combination having a 2–3 nm AlGaN layer followed by an AlInGaN layer. The purpose of incorporating the thin AlGaN layer was to keep the band offset at the heterointerface (barrier/GaN) constant, while controlling piezoelectric doping by incorporation of In into the top portion of the barrier. The total thickness of the AlInGaN and AlInGaN–AlGaN barriers were determined from scanning electron microscopy pictures and varied between 15 and 17 nm. The Al molar fraction in the barriers was determined from photoluminescence measurements and was approximately 12%.

The lattice mismatch in AlInGaN/GaN heterostructures with different In incorporation was studied by measuring the (0006) (Θ–2Θ) x-ray diffraction peaks arising from the AlInGaN barriers and the underlying GaN layers. These data show the AlInGaN–GaN heterostructures to be nearly lattice matched for an estimated In to Al ratio 5, which is in good agreement with the expectations based upon Vegard's law. This lattice match in our AlInGaN–GaN heterostructures
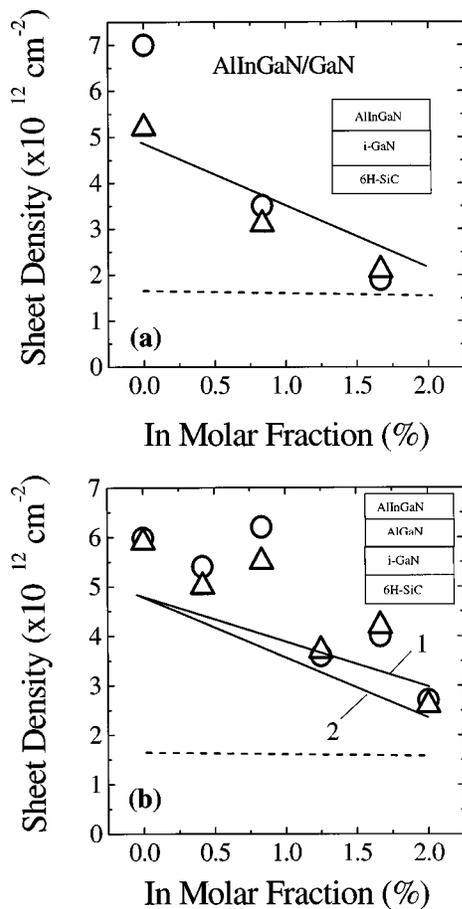
a)Electronic mail: gaskar@rpi.edu

FIG. 1. Measured (dots and triangles) and calculated (solid lines) sheet electron density in AlInGaN/GaN (a) and AlInGaN–AlGaN/GaN (b) heterostructures with 12% of Al and different incorporation of In. Lines 1 and 2 in (b) are calculated for the AlInGaN–AlGaN barrier with 3 and 1 nm of AlGaN, respectively. The total barrier thickness is 16 nm. Dashed lines show sheet density calculated for AlInGaN/GaN heterostructures without piezoelectric doping (spontaneous polarization only). Open circles correspond to sheet densities measured at room temperature, triangles correspond to $T = 80$ K. Insets show schematic epilayer designs of heterostructures.

FIG. 2. (a) Electron Hall mobility in AlInGaN/GaN heterostructures with 12% of Al and different molar fractions of In measured at $T = 80$ K; (b) calculated conduction-band diagrams for AlInGaN/GaN heterostructures with 12% of Al and different In content. Curve (1) corresponds to zero In incorporation; (2) In $= 1\%$; and (3) 2%. Dotted, dotted-dashed, and dashed lines mark Fermi-level positions for 1, 2, and 3, respectively. Thick solid lines show ground energy levels inside triangle quantum wells; (c) Hall mobility vs sheet density in (AlInGaN–AlGaN)/GaN at 77 K (solid dots), gated AlGaN/GaN heterostructures at 4.2 K (open circles), and AlGaN/GaN heterostructures with different doping at 77 K (triangles).

with 12% Al and 2% In should, in principle, nearly eliminate the piezoelectric doping.

Figure 1 shows the sheet electron density in AlInGaN/GaN and (AlInGaN–AlGaN)/GaN heterostructures, extracted from Hall measurements at room temperature and at 80 K. As seen from Fig. 1, the incorporation of In reduces the 2D electron density n_s in both heterostructure types. The sheet density decreases from approximately $6 \times 10^{12} \, \text{cm}^{-2}$ for heterostructures with zero In content (AlGaN/GaN structures) to $n_s = 2 – 2.5 \times 10^{12} \, \text{cm}^{-2}$ for the structures with 2% of In. The dependence of n_s on the In molar fraction is nearly the same for the heterostructures with and without the 2–3-nm-thick AlGaN layer in the barrier region. This result points to a very small change in the conduction-band offset caused by the incorporation of up to 2% of In, which is in good agreement with the expectations based on Vegard's law. Therefore, we attribute the decrease in n_s primarily to the reduction of the lattice mismatch and of the associated strain between the AlInGaN barrier and the GaN channel layer. From our measurements of n_s we thus estimate the contribution of piezoelectric doping in our structures to be approximately $4 \times 10^{12} \, \text{cm}^{-2}$.

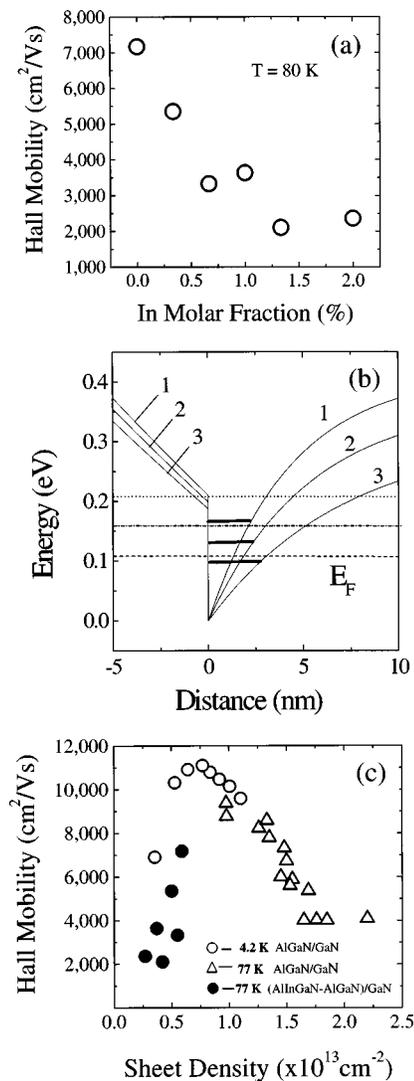In order to evaluate the contributions of both piezoelec-

tric and pyroelectric (spontaneous polarization) doping, we compared the experimental data with the calculated values of n_s shown by solid lines in Fig. 1. These calculations for $Al_{0.12}In_yGa_{1-0.12-y}N/GaN$ [Fig. 1(a)] and $Al_{0.12}In_yGa_{1-0.12-y}N/Al_{0.12}Ga_{0.88}N/GaN$ [Fig. 1(b)] took into account both pyroelectric and piezoelectric effects. The parameters used in the calculations are listed in Table I. The calculated values of n_s including only the piezo and the spontaneous polarization are close to the measured values indicating the piezoelectric and pyroelectric effects to be the only major contributors to 2D electron gas. This is expected as the background sheet carrier density due to unintentional doping of our barrier (AlInGaN) and the channel semi-insulating GaN layer was measured to be not more than $10^{12} \, \text{cm}^{-2}$. (These background measurements were made on thick individual layers.) Also, the calculated sheet electron

TABLE I. AlInGaN/GaN parameters used in our calculations.

Parameter	Units	Our value
Total barrier thickness (L)	nm	16
Thickness of AlGaN (L1)	nm	0–3
Thickness of InAlGaN (L2)	nm	13–16
Donor concentration in GaN	cm^{-3}	10^{15}
Donor concentration in AlGaN	cm^{-3}	3×10^{17}
Al concentration	%	12
Lattice constant	nm	$0.3548y + .3112x + .3189(1-x-y)$
Schottky barrier	eV	$1.3x + 0.84$
e_{33}	C/m^2	$0.97y + 1 - y - x + 1.55x$
e_{31}	C/m^2	$-0.36(1-y-x) - 0.58x - 0.57y$
c_{33}	GPa	$200y + 389x + 267*(1-x-y)$
c_{13}	GPa	$94y + 99x + 158(1-x-y)$
$In_yAl_xGa_{1-y-x}N$/GaN conduction-band discontinuity	eV	$0.75 \Delta Eg$
$In_yAl_xGa_{1-y-x}N$ band gap	eV	$1.9y + 3.4*(1-y-x) + 6.2x$
$In_yAl_xGa_{1-y-x}N$ spontaneous polarization at zero strain	C/m^2	$-0.052*x - 0.029$
Dielectric constant of AlN		8.5

density reduces from approximately 5×10^{12} cm^{-2} for AlGaN/GaN heterostructures (In=0) to 2.7×10^{12} cm^{-2} for (AlInGaN–AlGaN)/GaN and 2.4×10^{12} cm^{-2} for AlInGaN/GaN heterostructures with up to 2% of In. Thus, the calculated contribution of the piezoelectric effects (piezoelectric doping) is approximately 2.5×10^{12} cm^{-2}, which is about 30% less than measured experimentally. As can be seen from Fig. 1, our calculations also confirm a considerable contribution from the spontaneous polarization. We should emphasize that the total contribution of the spontaneous polarization to the electron sheet density charge is larger than 1.6×10^{12} cm^{-2} shown in Fig. 1 by dashed lines. A large fraction of the spontaneous polarization charge (approximately $2 – 2.5 \times 10^{12}$ cm^{-2}) compensates the depletion charge that would have existed in a totally undoped structure with no polarization or piezoelectric effects. Therefore, the contributions from the piezoelectric and pyroelectric charges are comparable at 0% of the indium molar fraction.

The reduction of strain in AlInGaN/GaN heterostructures with the incorporation of In not only decreases piezoelectric doping, but also strongly reduces 2D electron mobility. The measured electron Hall mobility μ_H in (AlInGaN–AlGaN)/GaN heterostructures at 80 K is shown in Fig. 2(a). The incorporation of 2% of In reduces the mobility by more than a factor of 3, from 7300 cm^2/V s (In=0%) to approximately 2000 cm^2/V s (In=2%). Nearly the same reduction in 80 K Hall mobility was also measured for (AlInGaN/GaN) heterostructures. At 300 K, the mobility in (AlInGaN–AlGaN)/GaN heterostructures decreased by half from 1200 cm^2/V s for zero In to 600 cm^2/V s for 2% of In. We attribute this reduction of Hall mobility in AlInGaN/GaN heterostructures to the suppression of the piezoelectric effects and of the associated piezoelectric doping. An additional factor is the decrease in screening of the ionized impurity scattering with

the decrease of n_s. Figure 2(b) shows the calculated band diagrams of AlInGaN/GaN heterostructures with different In content. As seen, the ground-state energy and Fermi level in the triangular quantum wells near the AlInGaN/GaN heterointerface with higher In content are in the regions of lower electric field (proportional to the band bending) and, thus, of lower quantization. As a result, electrons are becoming less 2D and more bulklike with lower mobility. Note that the measured decrease in Hall mobility with decrease in sheet electron density from the loss of piezoelectric doping in our nearly lattice-matched AlInGaN/GaN heterostructures is in good agreement with $\mu_H(n_s)$ data obtained in AlGaN/GaN heterostructures. In Fig. 2(c) we include 2D Hall mobility (at 80 K) as a function of sheet electron density in our (AlInGaN–AlGaN)/GaN heterostructures (present study) with that for AlGaN/GaN heterostructures from Ref. 10. Our results, therefore, clearly show the important role of the piezoelectric effects in both doping and the transport properties of 2D electron gas in AlInGaN–GaN heterojunctions.

In conclusion, we employed the strain energy-band engineering approach in order to demonstrate the influence of piezoelectric effects in AlInGaN/GaN heterostructures with different In content. The calculated results show that the contribution to 2D electron gas from the spontaneous polarization is approximately equal to the piezoelectric charge. The piezoelectric doping not only changes the sheet electron density but also strongly affects the transport properties of 2D electron gas. The obtained results show that in AlGaN/GaN heterostructures with 12% of Al, the piezoelectric effects increase the sheet density times mobility product $n_s\mu$ at room temperature by a factor of 5.

[1] A. Bykhovski, B. Gelmont, and M. Shur, J. Appl. Phys. **74**, 6734 (1993).
[2] A. D. Bykhovski, V. V. Kaminski, M. S. Shur, Q. C. Chen, and M. A. Khan, Appl. Phys. Lett. **69**, 3254 (1996).
[3] M. S. Shur, A. D. Bykhovski, and R. Gaska, MRS Internet J. Nitride Semicond. Res. **4S1**, G1.6 (1999).
[4] R. Gaska, A. D. Bykhovski, M. S. Shur, J. Yang, and A. Osinsky, Appl. Phys. Lett. **71**, 3673 (1997).
[5] N. Maeda, T. Nishida, N. Kobayashi, and M. Tomizawa, Appl. Phys. Lett. **73**, 1856 (1998).
[6] P. M. Asbeck, E. T. Yu, S. S. Lau, G. J. Sullivan, J. Van Hove, and J. M. Redwing, Electron. Lett. **33**, 1230 (1997).
[7] F. Bernardini, V. Fiorentini, and D. Vanderbilt, Phys. Rev. B **56**, 10024 (1997).
[8] A. D. Bykhovski, R. Gaska, and M. S. Shur, Appl. Phys. Lett. **73**, 3577 (1998).
[9] V. M. Fridkin, *Ferroelectrics–Semiconductors* (Nauka, Moscow, Russia, 1976), p. 90.
[10] R. Gaska, M. S. Shur, A. Bykhovski, A. O. Orlov, and G. L. Snider, Appl. Phys. Lett. **74**, 287 (1999).